

2

DTIC FILE COPY

MTL TR 89-72

AD

AD-A212 094

A C°-ANISOPARAMETRIC THREE-NODE SHALLOW SHELL ELEMENT FOR GENERAL SHELL ANALYSIS

ALEXANDER TESSLER
MECHANICS AND STRUCTURES BRANCH

August 1989

Approved for public release; distribution unlimited.

DTIC
ELECTE
SEP 12 1989
S B D



US ARMY
LABORATORY COMMAND
MATERIALS TECHNOLOGY LABORATORY

89 9 11 074

U.S. ARMY MATERIALS TECHNOLOGY LABORATORY
Watertown, Massachusetts 02172-0001

UNCLASSIFIED

SECURITY CLASSIFICATION OF THIS PAGE (When Data Entered)

REPORT DOCUMENTATION PAGE		READ INSTRUCTIONS BEFORE COMPLETING FORM
1. REPORT NUMBER MTL TR 89-72	2. GOVT ACCESSION NO.	3. RECIPIENT'S CATALOG NUMBER
4. TITLE (and Subtitle) A C ⁰ -ANISOPARAMETRIC THREE-NODE SHALLOW SHELL ELEMENT FOR GENERAL SHELL ANALYSIS		5. TYPE OF REPORT & PERIOD COVERED Final Report
7. AUTHOR(s) Alexander Tessler		6. PERFORMING ORG. REPORT NUMBER
9. PERFORMING ORGANIZATION NAME AND ADDRESS U.S. Army Materials Technology Laboratory Watertown, Massachusetts 02172-0001 SLCMT-MRS		8. CONTRACT OR GRANT NUMBER(s)
11. CONTROLLING OFFICE NAME AND ADDRESS U.S. Army Laboratory Command 2800 Powder Mill Road Adelphi, Maryland 20783-1145		10. PROGRAM ELEMENT, PROJECT, TASK AREA & WORK UNIT NUMBERS D/A Project: 1L161102.AH42 AMCMS Code: 61102A
14. MONITORING AGENCY NAME & ADDRESS (if different from Controlling Office)		12. REPORT DATE August 1989
		13. NUMBER OF PAGES 19
		15. SECURITY CLASS. (of this report) Unclassified
16. DISTRIBUTION STATEMENT (of this Report) Approved for public release; distribution unlimited.		15a. DECLASSIFICATION/DOWNGRADING SCHEDULE
17. DISTRIBUTION STATEMENT (of the abstract entered in Block 20, if different from Report)		
18. SUPPLEMENTARY NOTES		
19. KEY WORDS (Continue on reverse side if necessary and identify by block number) Shallow shell Kirchhoff regime Mindlin theory Penalty relaxation Marguerre theory Edge constraints Finite element Three-node triangle Anisoparametric functions		
20. ABSTRACT (Continue on reverse side if necessary and identify by block number) <p style="text-align: center;">(SEE REVERSE SIDE)</p>		

Block No. 20

ABSTRACT

A highly desirable three-node shallowly curved shell element is proposed for general shell analysis. Constrained-type C^0 -anisoparametric interpolations are derived for the membrane and transverse displacement fields by the use of explicit edge constraints. Pertinent issues on shell theory and finite element approximations are addressed. Several numerical studies are carried out which demonstrate the effectiveness of this new triangular element in the regime of thin and moderately thick shells.

CONTENTS

	Page
INTRODUCTION	1
FINITE ELEMENT ISSUES	3
Review of Penalty Relaxation Concept	4
Anisoparametric Interpolation Scheme	5
NUMERICAL EXAMPLES	8
CONCLUSIONS	15
REFERENCES	16



Accession For	
NTIS GRA&I	<input checked="" type="checkbox"/>
DTIC TAB	<input type="checkbox"/>
Unannounced	<input type="checkbox"/>
Justification	
By _____	
Distribution/ _____	
Availability Codes	
Dist	Avail and/or Special
A-1	

INTRODUCTION

The search for "optimal" shell finite elements has been underway for nearly two decades. In recent years, it has further accelerated in light of significant progress in the technology of shear-deformable C^0 bending elements (e.g., References 1-19). Although the main obstacles for these developments, known as shear and membrane locking phenomena, have been addressed extensively and several remedial schemes have been proposed, a viable three-node doubly curved shear-deformable element, which is the most desirable element for general shell analysis, has not yet been developed. The purpose of this effort is to derive such an element.

We base our finite element derivation upon Reissner-Mindlin plate theory which will constitute the bending part of the element. To account for the membrane deformations and the membrane-bending coupling associated with the shell-element curvatures, we shall resort to Marguerre's shallow shell equations. Shallow shell elements of this type specialized to the axisymmetric response proved effective in discretizing shallow as well as deep shell structures.¹² The major advantage of this analytic approach over general shell formulations (e.g., References 5 and 18) is its inherent simplicity. Herein, the displacements and stress resultants are attributed to the element reference plane. Consequently, integrations are carried out across the reference plane rather than the curved surface as in the general shell elements.

According to Reissner-Mindlin theory,²⁰⁻²² the strain-displacement relations can be expressed as:

$$\kappa = \{\kappa_{xx}, \kappa_{yy}, \kappa_{xy}\}^T = L_1(\theta) \quad (1)$$

$$\gamma = \{\gamma_{xz}, \gamma_{yz}\}^T = L_2(w) + I\theta \quad (2)$$

where κ and γ are, respectively, the curvature and transverse shear strain vectors, θ is the bending rotation vector

$$\theta^T = \{\theta_y, \theta_x\} \quad (3)$$

with θ_x and θ_y denoting the bending rotations about the x and y axes, respectively, w is the transverse displacement (refer to Figure 1), and the superscript T denotes transpose; L_1 and L_2 are the linear differential operators, and I is an identity matrix:

$$L_1 = \begin{bmatrix} \frac{\partial}{\partial x} & 0 \\ 0 & \frac{\partial}{\partial y} \\ \frac{\partial}{\partial y} & \frac{\partial}{\partial x} \end{bmatrix}, \quad L_2 = \begin{bmatrix} \frac{\partial}{\partial x} \\ \frac{\partial}{\partial y} \end{bmatrix}, \quad I = \begin{bmatrix} 1 & 0 \\ 0 & 1 \end{bmatrix}. \quad (4)$$

The Marguerre membrane strain-displacement relations for a **thin** shallow shell have the form:²³

$$\epsilon = L_1(u) + L_1(\xi)L_2(w) \quad (5)$$

with

$$u^T = \{u, v\} \quad (6)$$

where u and v are the membrane displacements in the x and y coordinate directions, respectively; and $\xi = \xi(x, y)$ is the initial height of the shallow shell.

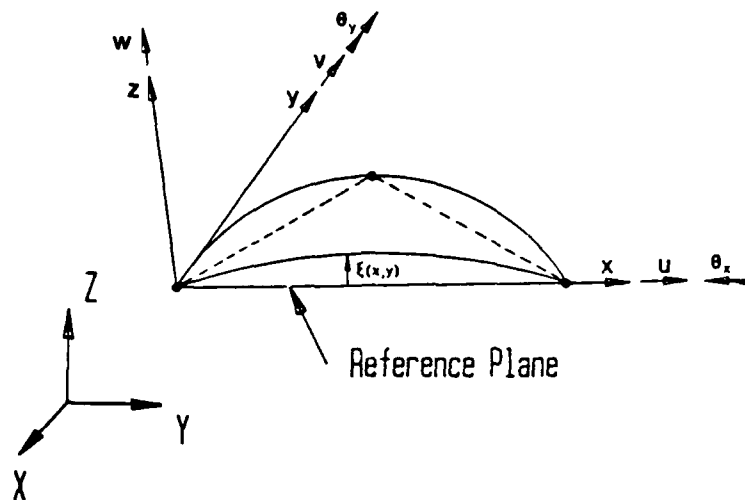


Figure 1. Shallow shell notation.

One important aspect, which in previous attempts to merge Reissner-Mindlin and Marguerre theories has not been addressed,⁹⁻¹² is the conceptual difference in the transverse displacement variables appearing in Equations 2 and 5. In Equation 2, w is a weighted average transverse displacement across the thickness, whereas in Equation 5, w represents the mid-surface transverse displacement. The former variable comes into play due to the inclusion of shear deformation in Reissner-Mindlin theory; the latter one is a consequence of the Kirchhoff thin-regime assumption, which neglects shear deformation. Utilizing Equation 2, the Kirchhoff thinness constraint reads:

$$\mathbf{L}_2(\mathbf{w}) = -\mathbf{I}\theta. \quad (7)$$

Replacing Equation 7 into Equation 5 yields the Marguerre membrane strains consistent with the Reissner-Mindlin strains:

$$\boldsymbol{\epsilon} = \mathbf{L}_1(\mathbf{u}) - \mathbf{L}_1(\xi)\theta. \quad (8)$$

The stress resultants, which are attributed to the reference plane of the shell, are related to the strains through the constitutive law:

$$\mathbf{N} = \{N_{xx}, N_{yy}, N_{xy}\}^T = \mathbf{A}\boldsymbol{\epsilon} \quad (9)$$

$$\mathbf{M} = \{M_{xx}, M_{yy}, M_{xy}\}^T = \mathbf{D}\boldsymbol{\kappa} \quad (10)$$

$$\mathbf{Q} = \{Q_x, Q_y\}^T = \mathbf{G}\boldsymbol{\gamma} \quad (11)$$

where \mathbf{A} , \mathbf{D} , and \mathbf{G} are, respectively, the membrane, bending, and transverse shear constitutive matrices. For an isotropic shell of constant thickness, t , the constitutive matrices are given by:

$$\mathbf{A} = \frac{E t}{(1-\nu^2)} \begin{bmatrix} 1 & \nu & 0 \\ & 1 & 0 \\ \text{sym.} & & \frac{1}{2}(1-\nu) \end{bmatrix}, \quad \mathbf{D} = \frac{t^2}{12} \mathbf{A}, \quad (11a)$$

$$\mathbf{G} = k^2 t \mathbf{G} \begin{bmatrix} 1 & 0 \\ 0 & 1 \end{bmatrix}$$

where E is Young's modulus, G is the shear modulus, and ν is Poisson's ratio; $k^2 = 5/6$ is Reissner's shear correction factor.²⁰

The principle of virtual work can then be employed to derive the finite element stiffness equilibrium equations:

$$\iint_A (\mathbf{N}^T \delta \boldsymbol{\epsilon} + \mathbf{M}^T \delta \boldsymbol{\kappa} + \mathbf{Q}^T \delta \boldsymbol{\gamma} - q \delta w) dA = 0 \quad (12)$$

where q is the distributed transverse loading, A is the reference plane area, and δ denotes the variational operator.

FINITE ELEMENT ISSUES

The development of effective curved shear-deformable shell elements is severely hampered by the "locking phenomena" (extreme stiffening), reflecting the inability of the shell to bend without stretching ("membrane locking") and transverse shearing ("shear locking"). The two phenomena are directly linked to the penalized strain energy which, in its nondimensional form, can be expressed as:

$$U(\boldsymbol{\kappa}, \boldsymbol{\gamma}, \boldsymbol{\epsilon}) = U_b(\boldsymbol{\kappa}) + \alpha_s U_s(\boldsymbol{\gamma}) + \alpha_m U_m(\boldsymbol{\epsilon}) \quad (13)$$

in which $U_b(\boldsymbol{\kappa})$, $U_s(\boldsymbol{\gamma})$, and $U_m(\boldsymbol{\epsilon})$ denote the nondimensional bending, transverse shear, and membrane energy integrals; and α_s and α_m are the nondimensional shear and membrane penalty parameters, respectively. Note that $\alpha_s = O(\lambda^2/t^2)$ and $\alpha_m = O[(\kappa_\xi \lambda^2)^2/t^2]$, where λ and κ_ξ are, respectively, some characteristic span and curvature of the shallow shell.^{11,12} As the shell thickness, t , diminishes to zero, both α_s and α_m approach infinity, thereby enforcing the vanishing shear and membrane strains:

$$\mathbf{L}_2(\mathbf{w}) \rightarrow -\mathbf{I}\boldsymbol{\theta} \quad (\text{Kirchhoff constraints}) \quad (14a)$$

$$\mathbf{L}_1(\mathbf{u}) \rightarrow \mathbf{L}_1(\boldsymbol{\xi})\boldsymbol{\theta} \quad (\text{Membrane inextensibility constraints}). \quad (14b)$$

The particular appeal of this theory is that the variational statement, Equation 12, requires a class of C^0 continuous approximations for the w , \mathbf{u} , and $\boldsymbol{\theta}$ fields (since their highest spatial derivative in Equation 12 is of order one) and, therefore, simple shape functions can be used. On the other hand, constraints, Equation 14, when imposed at the element level, pose severe limitations on the kinematic freedom attainable by each element, often resulting in shear and/or membrane locking.

For a successful discretization of the theory, a consistent resolution of the locking deficiencies must be sought. In Reference 4, we have elaborated on an approximation strategy dealing effectively with the aforementioned difficulties, which involves a redefinition of the penalty parameters to allow relaxation of Equation 14 at the element level and an implementation of appropriate interpolation schemes which may best accommodate Equation 14. We shall pursue both of these avenues in deriving our three-node shallow shell element.

Review of Penalty Relaxation Concept

The first facet of our approximating strategy deals with the issue of relaxing the enforcement of penalty constraints at the element level.

Concurrently with the element displacement approximations denoted as w^h , u^h , and θ^h (henceforth, h signifies a characteristic length scale of the discretization), we approximate the constitutive matrices A and G by incorporating the "element penalty relaxation" parameters:

$$N^h = \phi_m^2 A \epsilon^h, \quad Q^h = \phi_s^2 G \gamma^h, \quad M^h = D \kappa^h \quad (15)$$

where the element strains are

$$\epsilon^h = L_1(u^h) - L_1(\xi)\theta^h, \quad \gamma^h = L_2(w^h) + I\theta^h, \quad \kappa^h = L_1(\theta^h) \quad (16)$$

and the penalty relaxation parameters are nondimensional positive quantities of the form:

$$\phi_i^2 = (1 + C_i \alpha_i)^{-1} \quad (i = m, s) \quad (17)$$

where C_i are positive element constants, and α_i are element analytic penalty parameters. Note that $\alpha_s = O(h^2/t^2)$ and $\alpha_m = O[(\kappa_\xi^h h^2)/t^2]$, where κ_ξ^h represents some characteristic initial curvature of the element. The corresponding principle of virtual work for a single element approximation takes the form:

$$\iint_{A^e} [(N^h)^T \delta \epsilon^h + (M^h)^T \delta \kappa^h + (Q^h)^T \delta \gamma^h - q \delta w^h] dA = 0 \quad (18)$$

where integration extends over the element reference plane with A^e denoting the element reference area. The resulting element strain energy appears in the basic form of Equation 13, except that all quantities are superscribed with h (i.e., element approximations); however, the element penalty parameters take a fundamentally different form:

$$\alpha_i^h = \alpha_i / (1 + C_i \alpha_i) \quad (i = m, s). \quad (19)$$

An heuristic argument in support of Equation 19 may be stated as follows. As $t \rightarrow 0$, some degree of relaxation of constraints, Equation 14, may be expected as now α_i^h approach finite penalty values C_i^{-1} , which for low order elements are of $O(1)$.⁴ These thin-regime penalty numbers (C_i^{-1}) can be seen to be element/interpolation dependent. Thus, higher order kinematic interpolations may necessitate larger C_i^{-1} (i.e., smaller C_i), which will ensure stricter element-level enforcement of the vanishing penalty constraints, Equation 14. Conversely, low order kinematic interpolations may require smaller C_i^{-1} to allow for greater element-level relaxation of Equation 14. Clearly, in the limiting case when the element kinematic freedoms are

sufficient to capture the exact solution of the problem, C_i^{-1} can be very large (or simply, $C_i = 0$), in which case Equation 19 takes on the analytic (unrelaxed) form.

From a practical computational perspective, C_i can simply be selected once and for all (for a particular element) from a rather limited series of numerical tests. As the kinematic approximations improve with the h-refinement (i.e., as $h \rightarrow 0$, $\kappa_\xi^h \rightarrow 0$), α_i^h approach their analytic values α_i , thus ensuring convergence to the "true" solution both in the constitutive and kinematic sense.^{4,8,11,12} As will be demonstrated by our numerical examples, the penalty parameter of Equation 19 is responsible for removing whatever spurious constraining may have existed in the "unrelaxed" element kinematics.

Anisoparametric Interpolation Scheme

A complementary means for enhancing element behavior is by way of appropriate kinematic interpolations, termed anisoparametric,¹³ which can best accommodate the requirements of Equation 14. The anisoparametric strategy suggests distinctly different degree polynomials for w , θ , and u to reflect the differences in the order of the differential operators L_2 and I in Equation 14a and, likewise, L_1 and $L_1(\xi)$ in Equation 14b. (These contrast the well-established isoparametric interpolations; identical degree polynomials for all kinematic variables.) The specific aim is to **design out** the unwanted "spurious" constraint equations that may arise from Equation 14.

To represent the bending part of the shell element, we adopt the three-node anisoparametric plate element,^{13,14} in which θ_x and θ_y are interpolated linearly, while w is represented by a complete quadratic polynomial; throughout the formulation, area-parametric coordinates $\zeta = (\zeta_1, \zeta_2, \zeta_3)$ are used as a basis for all interpolations (refer to Figure 2):

$$\theta_I^h = \mathbf{N}^{(1)} \theta_I^h \quad (I=x,y), \quad w^h = \mathbf{N}^{(2)} w^h \quad (20)$$

where $\mathbf{N}^{(1)}$ and $\mathbf{N}^{(2)}$ are the row vectors of linear and quadratic shape functions, respectively, and

$$(\theta_I^h)^T = \{\theta_{Ij}^h\}, \quad (w^h)^T = \{w_k^h\} \quad (I=x,y; j=1,2,3; k=1,\dots,6) \quad (21)$$

are the vectors of nodal dof.

Adopting the shell element of constant curvature [i.e., interpolating $\xi^h(\zeta)$ parabolically], constraints, Equation 14b, necessitate a complete 10-term cubic polynomial for the u and v displacements:

$$u^h = \mathbf{N}^{(3)} u^h, \quad v^h = \mathbf{N}^{(3)} v^h \quad (22)$$

where $\mathbf{N}^{(3)}$ is a row vector of cubic shape functions, and

$$(u^h)^T = \{u_k^h\}, \quad (v^h)^T = \{v_k^h\} \quad (k=1,\dots,10) \quad (23)$$

are the vectors of nodal dof.

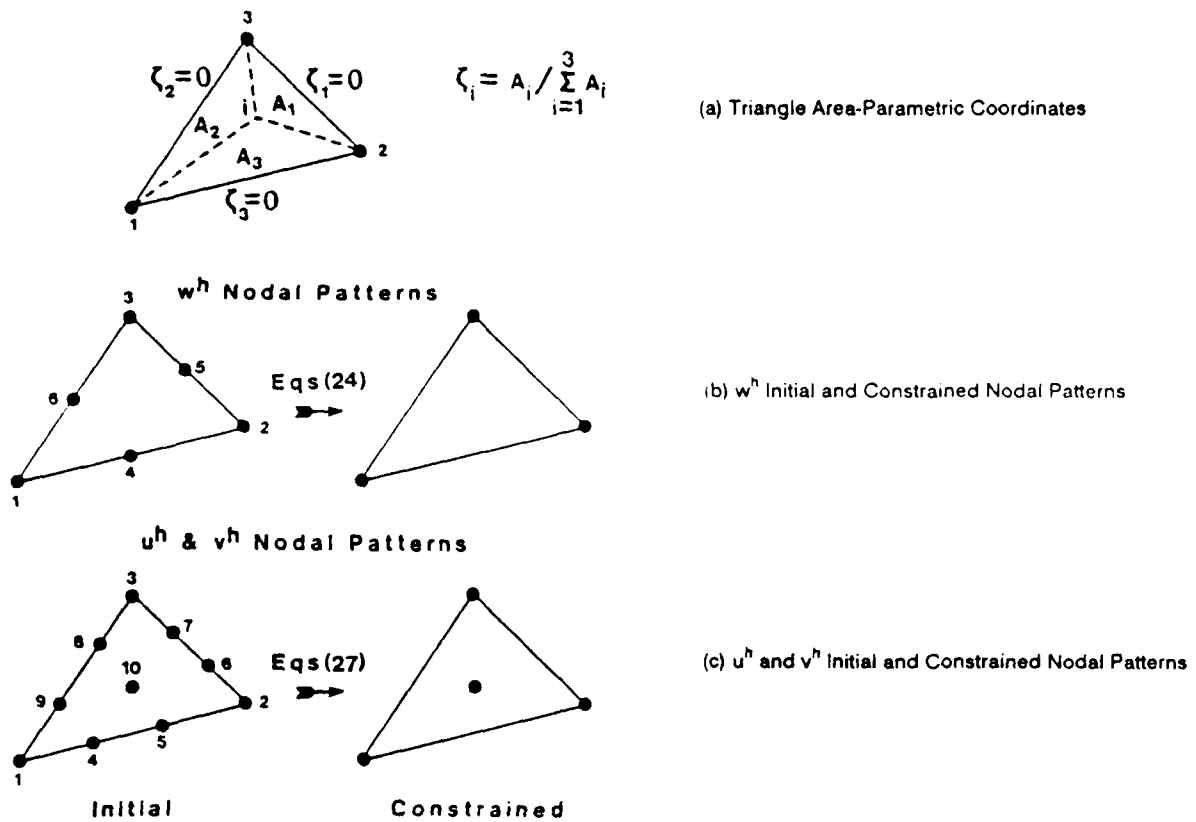


Figure 2.

Evidently, the anisoparametric interpolations produce the same degree polynomial representations for the left- and right-hand sides of the constraint equations, Equation 14; the condition that is paramount to improving element behavior in the vanishing thickness regime.

Edge Shear Constraints

Although the initial w^h rests on six w^h dof (i.e., three corner and three midedge dof), a kinematically consistent elimination of the midedge dof is possible a priori to the element stiffness derivation. To obtain a three-node pattern, w^h can be constrained by the one-dimensional edge constraints:

$$\gamma_{sz,s}^{(k)} = \frac{\partial}{\partial s} \left[w^h(s),_s + \theta_n^h(s) \right] = 0 \quad (k=1,2,3) \quad (24)$$

where s denotes a coordinate running along the k^{th} edge of the triangular element reference plane; and $\theta_n^h(s)$ is the tangential edge rotation which is related to $\theta_x^h(s)$ and $\theta_y^h(s)$ via an orthogonal transformation. From Equation 24, there results three decoupled equations in terms of the midedge w^h dof, which give rise to the constraints:

$$w_c^h = W_o w^h + W_x \theta_x^h + W_y \theta_y^h \quad (25)$$

where W_q ($q = o, x, y$) are 3×3 transformation matrices, and

$$(\mathbf{w}_c^h)^T = \{\mathbf{w}_{j+3}^h\}, \quad (\mathbf{w}^h)^T = \{\mathbf{w}_j^h\} \quad (j=1,2,3). \quad (26)$$

Upon substituting Equation 25 into Equation 20, we obtain a three-node interpolation for the transverse displacement.

Edge Membrane Constraints

In the manner analogous to the above dof reduction for w^h , one-dimensional edge constraints can be devised to condense out the intraedge u^h and v^h dof. The following constraint equations provide four edge-compatible relations for each edge:

$$\frac{\partial^p}{\partial s^p} \begin{bmatrix} \epsilon_s(s) \\ \gamma_{sn}(s) \end{bmatrix} \stackrel{(k)}{=} \frac{\partial^p}{\partial s^p} \begin{bmatrix} \underline{u}_s^h - \xi_s^h \theta_n^h \\ \underline{v}_s^h - \xi_n^h \theta_n^h - \xi_s^h \theta_s^h \end{bmatrix} \stackrel{(k)}{=} \mathbf{0} \quad (k=1,2,3; p=1,2) \quad (27)$$

where $u^h(s)$ and $v^h(s)$ are cubic displacement fields along and normal to the k -th edge, respectively, and

$$\xi_q^h \equiv \xi^h(\zeta)_q \quad \left| \quad \begin{array}{l} (q = s, n; k=1,2,3) \\ \zeta_k = 0 \end{array} \right. \quad (28)$$

are the k -th edge slopes.

By the use of appropriate orthogonal transformations, Equation 27 is expressed in terms of the shell element variables of interest, namely, u^h , v^h , θ_x^h and θ_y^h dof, and algebraically solved for the intraedge u^h and v^h dof:

$$\begin{aligned} \mathbf{u}_c^h &= \mathbf{U}_o \mathbf{u}^h + \mathbf{U}_x \theta_x^h + \mathbf{U}_y \theta_y^h \\ \mathbf{v}_c^h &= \mathbf{V}_o \mathbf{v}^h + \mathbf{V}_x \theta_x^h + \mathbf{V}_y \theta_y^h \end{aligned} \quad (29)$$

where

$$(\mathbf{u}_c^h)^T = \{\mathbf{u}_i^h\}, \quad (\mathbf{v}_c^h)^T = \{\mathbf{v}_i^h\} \quad (i=4, \dots, 9) \quad (30)$$

and \mathbf{U}_q and \mathbf{V}_q ($q = o, x, y$) are 6×3 transformation matrices. Equation 29 is substituted into the initial interpolations, Equation 22, to give the constrained fields for the membrane displacements in terms of the corner-node dof and two centroidal dof. The latter dof are condensed out statically after the formation of the element stiffness matrix and consistent load vector. Consequently, a three-node, 15 dof element pattern is achieved.

Note that the edge constraint procedures just described preserve the original polynomial order of the constrained variables (w^h , u^h , and v^h); moreover, one can show that the constrained fields are fully compatible across element edges, and they allow for rigid body motion

without straining. For further details on this procedure and for the explicit form of the shape functions, refer to references 13 and 14.

The remainder of the formulation follows standard finite element procedures. Application of the virtual work statement, Equation 18, while performing exact integration (normal quadrature rule,¹) throughout, yields the element stiffness equations. The issue of the rotational variable normal to the reference plane, θ_z^h , needed to prevent mathematical singularities in the global coordinates, produces three additional dof for the element (e.g., see Reference 10).

NUMERICAL EXAMPLES

An important step in completing the relaxation methodology of the Finite Element Issues Section is to obtain appropriate α_i parameters and the values for C_i ($i = m, s$). Herein, we adopt the approach developed in Reference 13, where α_i are defined as:

$$\alpha_i \equiv \Sigma k_i^\theta / \Sigma k_b^\theta \quad (i=s,m; \quad b - \text{bending}) \quad (31)$$

in which k_i^θ and k_b^θ denote the element diagonal stiffness coefficients associated with θ_x^h and θ_y^h dof for the unrelaxed case, i.e., $\phi_i^2 = 1$. As far as the "optimal" values for C_s and C_m , these are determined from numerical testing. The shear relaxation constant, $C_s = 2$, has already been established to ensure free of locking plate-element behavior;¹³ $C_m = 1$ was chosen from the numerical results of the present study.

The present element was tested on a series of challenging thin shell problems,^{24,25} and a moderately thin shell. To ascertain the influence of the membrane penalty relaxation and the membrane anisoparametric kinematic field upon element behavior, three versions of the element were tested. They are:

- MIN3: A facet triangle ($\kappa_\xi^h = 0$) with the shear relaxation ($C_s = 2$), possessing constant membrane strains, no membrane-bending coupling, and no membrane relaxation ($\phi_m^2 = 1$).
- MIN3S: A curved triangle with the shear relaxation only ($C_s = 2, C_m = 0$).
- MIN3SM: A curved element with both the shear and membrane relaxations ($C_s = 2, C_m = 1$).

Our findings are summarized as follows.

Test of Rigid-Body Motion: A spectral analysis was performed on the element stiffness matrix for the facet, singly curved, and doubly curved element geometry, to check MIN3's ability to move as a rigid body without incurring any straining. Under all conditions tested, there resulted six requisite zero eigenvalues associated with rigid body motion.

Thin Cantilevered Arch: A simple test of both membrane inextensibility and shearless deformation is a 90° thin circular arch clamped at one end and loaded by a bending moment at the other (Figure 3). An additional modeling difficulty here is that the arch is rather narrow (radius/thickness ratio: $R/t = 272$; width/thickness ratio: $B/t = 1$), hence the element aspect ratios are large. At all discretization levels, a constant value of the applied bending moment is recovered in each element, with all other stress resultants vanishing. Figure 4 depicts a convergence study of the tip bending rotation, which is also a direct measure of the

strain energy for this problem. Note that while MIN3S exhibits considerable membrane stiffening, MIN3 and MIN3SM experience no such difficulty, converging rather rapidly, with the facet element being slightly more flexible. Both MIN3 and MIN3SM yield results of acceptable engineering accuracy, even under coarse discretizations.

CANTILEVERED ARCH

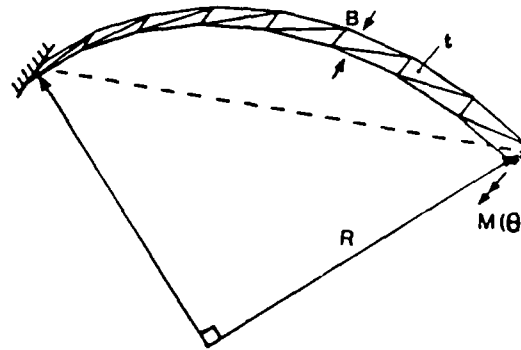


Figure 3. 90° thin cantilevered arch under tip moment ($R/t = 272$).

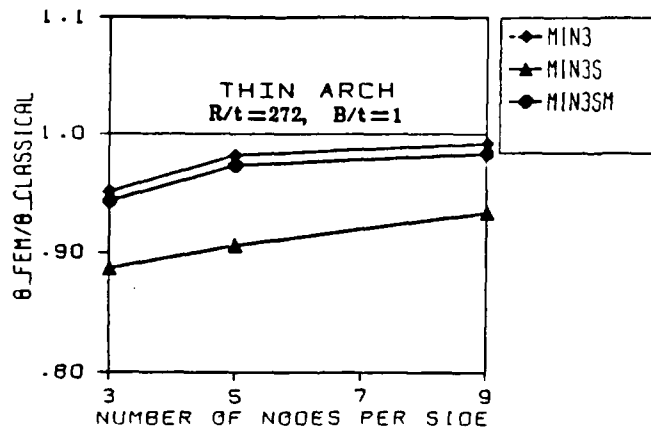


Figure 4. 90° thin cantilevered arch; convergence study of tip rotation under applied moment.

Open-Ended Pinched Cylinder: The open-ended cylindrical shell subjected to two radial forces 180 degrees apart (Figure 5) is a widely used test problem to establish how well a singly curved shell element can represent inextensional bending.^{1,5} As $t/R \rightarrow 0$, pure inextensional state of deformation is attained in the cylinder.

Figure 6 depicts a nine-node-per-side discretization (128 elements) and its deformed shape for a symmetric octant of the cylinder. Figures 7 and 8 show convergence studies of the deflection under the load for the moderately thin ($R/t = 50$) and thin ($R/t = 2000$) cylinders. The present results are compared with exact solutions and those obtained with three reduced and one fully integrated Reissner-Mindlin quadrilateral elements. These elements are:

- 9H-S2: Nine-node heterosis element with selective integration.

- 8S-U2: Eight-node serendipity element with uniform integration.
- 4L-S1: Four-node Lagrange element with selective integration.
- 16L-U4: Sixteen-node Lagrange fully integrated element.

For specific details on these elements and references thereof, refer to References 1 and 5.

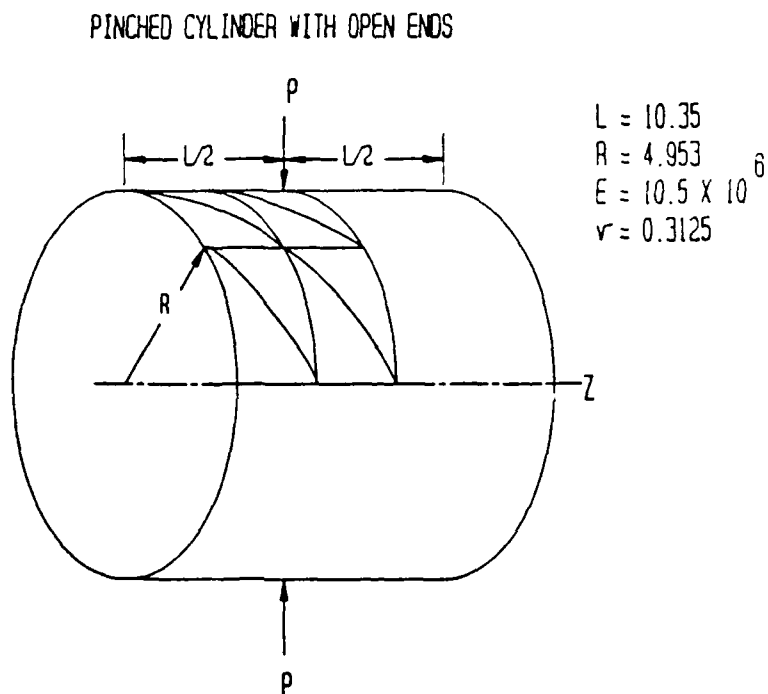


Figure 5. Pinched, open-ended circular cylinder.

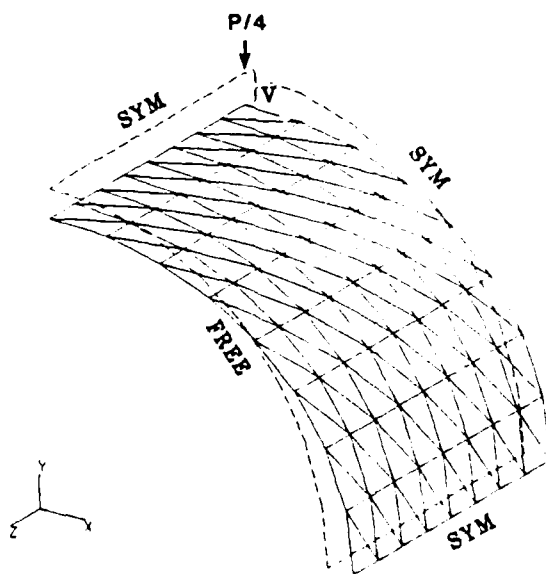


Figure 6. Pinched, open-ended circular cylinder; triangular element discretization for symmetric octant. Undeformed and deformed shapes.

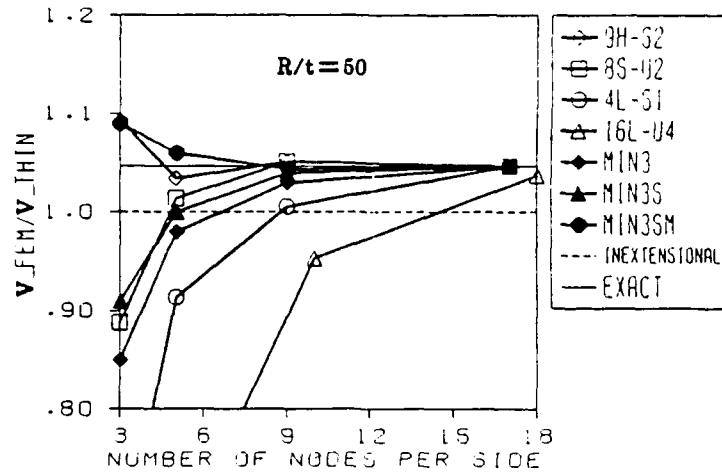


Figure 7. Moderately thin-pinned cylinder ($R/t = 50$); convergence study of tip displacement under applied force.

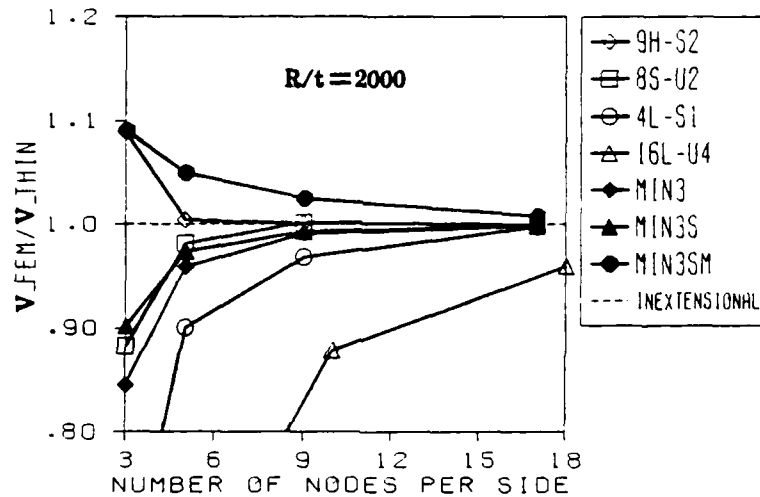


Figure 8. Thin-pinned cylinder ($R/t = 2000$); convergence study of tip displacement under applied force.

Clearly, all three MIN3 versions perform very well, with MIN3 being the stiffest of the three while MIN3SM exhibits the most flexible behavior. Evidently, MIN3SM is equally competitive with the best performing quadrilateral (9H-S2) for this problem.

Scordelis-Lo Roof: The geometric description, loading, and material data for this membrane-response dominated cylindrical shell are presented in Figure 9.²⁶ In Figure 10, a thirteen-node-per-side mesh and the corresponding deformed shape are shown for a symmetric quadrant of the shell. Figure 11 shows a convergence study of the vertical displacement at the midpoint of the free edge of the cylinder. The finite element displacement is normalized with respect to a converged numerical solution, $V = 0.3024$.²⁵

The results obtained with four different membrane-strain approximations for the Discrete Kirchhoff Triangle (DKT) element²⁷ (taken from Reference 25), are also included in this study. Note that DKT is strictly a thin bending element (no shear deformation included). Briefly, the four DKT elements are:

- DKT/CST: A facet triangle (no membrane/bending coupling) with constant membrane strains.
- DKT/CST*: A constant-strain triangle but which includes membrane/bending coupling via a membrane projection scheme.²⁸
- DKT/LST: A facet triangle (no membrane/bending coupling) which incorporates a linear membrane field and reduced integration of the membrane strain energy.²⁹
- DKT/OB: A facet triangle (no membrane/bending coupling) with a linear membrane field.³⁰

The best performing elements for this problem are DKT/OB, DKT/LST, and MIN3SM; DKT/CST and DKT/CST* exhibit considerable membrane stiffening, showing a very slow rate of convergence. Also note that MIN3 and MIN3S, although somewhat stiffer than MIN3SM, perform comparably and converge rapidly.

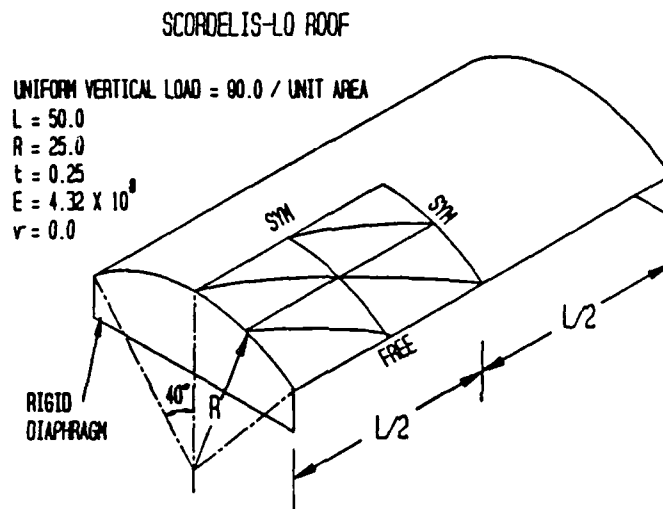


Figure 9. Scordelis-Lo roof; vaulted roof under dead uniform load supported by rigid diaphragms.

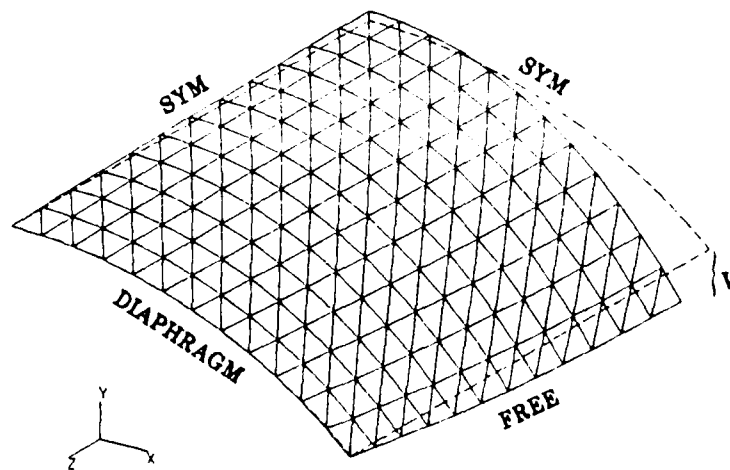


Figure 10. Scordelis-Lo roof; triangular element discretization for symmetric quadrant. Undeformed and deformed shapes.

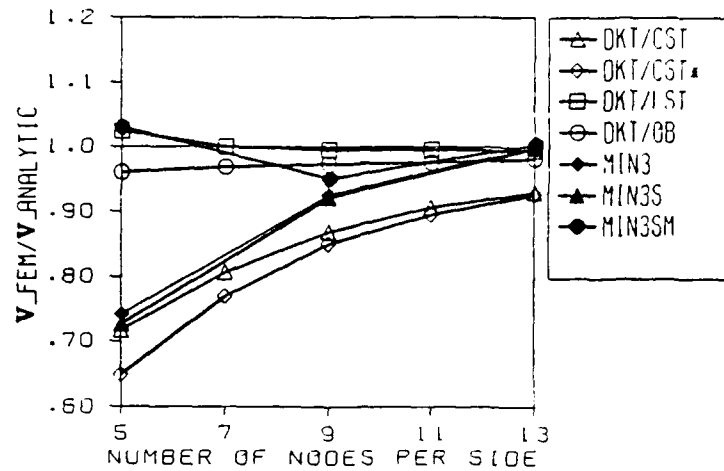


Figure 11. Scordelis-Lo roof; convergence study of vertical displacement at midpoint of free edge.

Pinched Hemisphere: A thin hemispherical shell under self-equilibrating radial forces is a rather challenging test problem for doubly curved shell elements.²⁵ The shell is in the state of near extensional bending, having large rigid-body rotations in the deformed configuration. Many commonly well-behaved elements, both of quadrilateral and triangular shapes, exhibit significant membrane stiffening when modeling this problem.^{5,25}

Figure 12 depicts a nine-node-per-side discretization of a symmetric quadrant of the hemisphere. Figure 13 shows a convergence study for the radial displacement under the applied force which is normalized with respect to an analytic solution.³¹ For comparison, results with the four DKT elements are also included. It is evident that both DKT/OB and MIN3S exhibit excessive membrane stiffening, while the other elements suffer no such deficiency and converge rapidly; MIN3SM again evolves as a reliable performer.

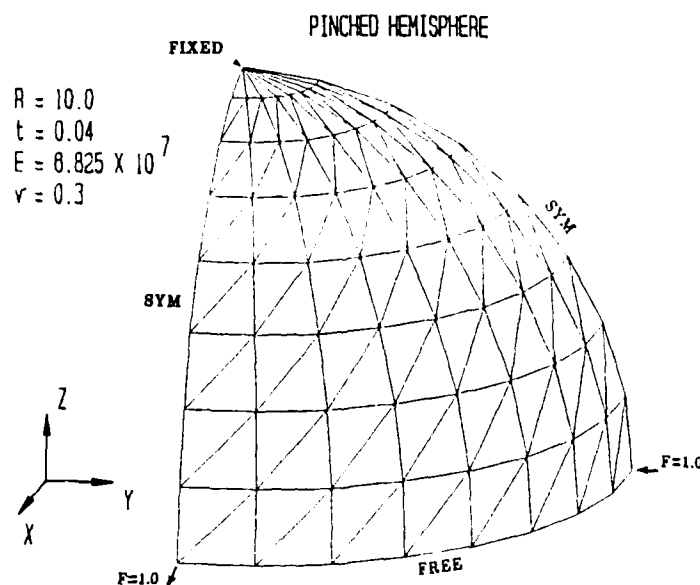


Figure 12. Pinched hemisphere; triangular element discretization for symmetric quadrant.

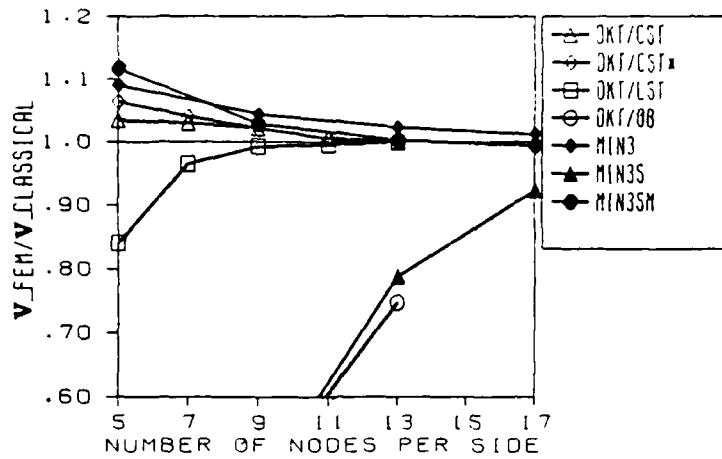


Figure 13. Pinched hemisphere; convergence study of displacement under applied force.

Semicircular Moderately Thick Arch: A moderately thick semicircular arch ($R/t = 8$), clamped at both ends and subject to a central vertical force (Figure 14), is known to exhibit significant membrane and shear deformations.¹¹ The arch can be analyzed, for example, using meshes for the pinched cylinder problem, with the appropriate boundary conditions and loading as shown in Figure 14. Additionally, to ensure the x-y plane deformations only, all out-of-plane global degrees of freedom are restrained in the model (i.e., $w = \theta_x = \theta_y = 0$). The analytic solution for the deflection under the load can be found in a straightforward manner according to the Timoshenko beam theory, and it will serve as a benchmark in studying convergence for this problem. Figure 15 shows convergence results for the deflection under the load, which is normalized with respect to the thin (inextensional) solution, V_{thin} . Also shown is the exact solution, $V_{exact} = 1.2015 V_{thin}$ (which includes shear and membrane deformations), and the extensional solution, $V_{exact} = 1.1299 V_{thin}$ (which ignores shear deformation). Note that all three element versions converge to the exact solution, with MIN3SM yielding the most accurate results.

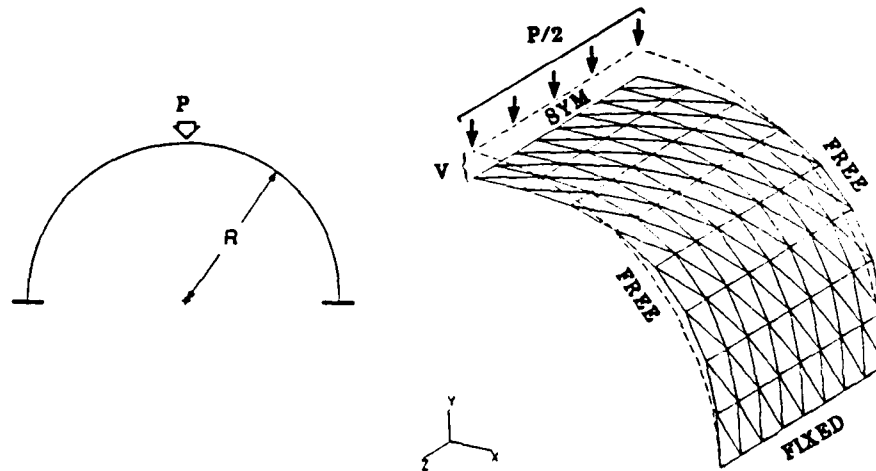


Figure 14. Semicircular moderately thick arch under vertical force ($R/t = 8$). Undeformed and deformed shapes.

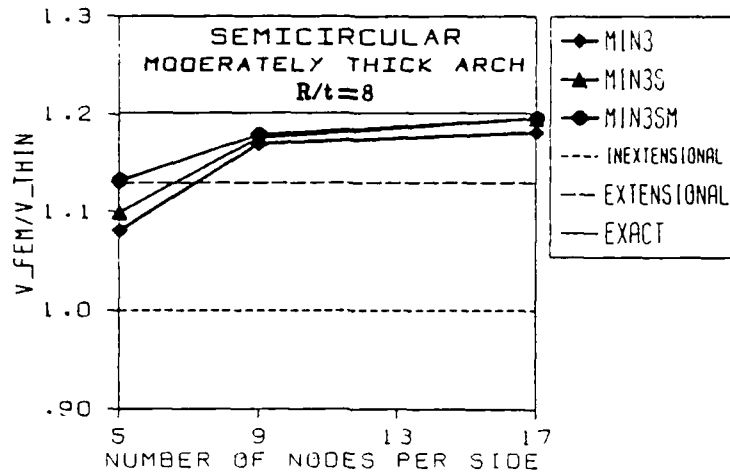


Figure 15. Semicircular moderately thick arch; convergence study of vertical displacement under applied force.

CONCLUSIONS

A three-node, constant curvature shallow shell element (MIN3SM) has been formulated by way of properly merging the Reissner-Mindlin theory of shear-deformable plates and Marguerre's shallow shell equations for the membrane strains. The issues of thin-regime shear and membrane locking have been addressed via shear and membrane penalty relaxation parameters and edge-constrained anisoparametric interpolations. The element is fully integrated and, hence, kinematically reliable; it possesses six requisite rigid-body modes and has no "spurious" zero-energy modes.

Solutions to several locking-sensitive singly and doubly curved thin shell problems have demonstrated the element's excellent modeling capabilities, devoid of both shear and membrane locking. Our numerical tests have shown that MIN3SM is consistently competitive with the best DKT elements. However, MIN3SM has a practical advantage of having a wider range of applicability which extends to moderately thick shells.

REFERENCES

1. HUGHES, T. J. R. The Finite Element Method: Linear Static and Dynamic Finite Element Analysis. Chapter 5, Prentice-Hall, N.J., 1987.
2. Finite Element Methods for Plate and Shell Structures, Vol. 1: Element Technology. T. J. R. Hughes and E. Hinton, ed., Pineridge Press, Swansea, U.K., 1986.
3. BELYTSCHKO, T. *A Review of Recent Developments in Plate and Shell Elements* in Computational Mechanics - Advances and Trends, A. K. Noor, ed., ASME, AMD, v. 75, NY, 1986, p. 217-231.
4. TESSLER, A. *Shear-Deformable Bending Elements with Penalty Relaxation* in Finite Element Methods for Plate and Shell Structures, Vol. 1: Element Technology, T. J. R. Hughes and E. Hinton, ed., Pineridge Press, Swansea, U.K., 1986, p. 266-290.
5. STANLEY, G. M. *Continuum-Based Shell Elements*. Ph.D. dissertation, Stanford University, 1985.
6. TESSLER, A., and DONG, S. B. *On a Hierarchy of Conforming Timoshenko Beam Elements*. Computers and Structures, v. 14, 1981, p. 335-344.
7. TESSLER, A. *An Efficient, Conforming Axisymmetric Shell Element Including Transverse Shear and Rotary Inertia*. Computers and Structures, v. 15, 1982, p. 567-574.
8. TESSLER, A., and HUGHES, T. J. R. *An Improved Treatment of Transverse Shear in the Mindlin-Type Four-Node Quadrilateral Element*. Comput. Meths. Appl. Mech. Engrg., v. 39, 1983, p. 311-335.
9. STOLARSKI, H., and BELYTSCHKO, T. *Shear and Membrane Locking in Curved C^0 Elements*. Computer Meths. Appl. Mech. Engrg., v. 41, 1983, p. 279-296.
10. CRISFIELD, M. A. Finite Elements and Solution Procedures for Structural Analysis, Vol. 1: Linear Analysis. Pineridge Press, Swansea, U.K., 1986.
11. TESSLER, A., and SPIRIDIGLIOZZI, L. *Curved Beam Elements with Penalty Relaxation*. Int. J. Numer. Meth. Engrg., v. 23, 1986, p. 2245-2262.
12. TESSLER, A., and SPIRIDIGLIOZZI, L. *Resolving Membrane and Shear Locking Phenomena in Curved Shear-Deformable Axisymmetric Shell Elements*. Int. J. Num. Meth. Engrg., v. 26, 1988, p. 1071-1086.
13. TESSLER, A., and HUGHES, T. J. R. *A Three-Node Mindlin Plate Element with Improved Transverse Shear*. Comput. Meths. Appl. Mech. Engrg., v. 50, 1985, p. 71-101.
14. TESSLER, A. *A Priori Identification of Shear Locking and Stiffening in Triangular Mindlin Elements*. Comput. Meths. Appl. Mech. Engrg., v. 53, 1985, p. 183-200.
15. RAMESH BABU, C., and PRATHAP, G. *A Field Consistent Two-Node Curved Axisymmetric Shell Element*. Int. J. Numer. Meth. Engrg., v. 23, 1986, p. 1245-1261.
16. FRIED, I., JOHNSON, A., and TESSLER, A. *Minimal-Degree Thin Triangular Plate and Shell Bending Finite Elements of Order Two and Four*. Comput. Meths. Appl. Mech. Engrg., v. 56, 1986, p. 283-307.
17. HINTON, E., and HUANG, H. C. *A Family of Quadrilateral Mindlin Plate Elements with Substitute Shear Strain Fields*. Computers and Structures, v. 33, 1986, p. 409-431.
18. BATHE, K. J., and DVORKIN, E. N. *A Formulation of General Shell Elements - The Use of Mixed Interpolation of Tensorial Components*. Int. J. Num. Meth. Engrg., v. 22, 1986, p. 697-722.
19. SALEEB, A. F., CHANG, T. Y., and YINGYEUNYONG, S. *A Mixed Formulation of C^0 -Linear Triangular Plate/Shell Element - the Role of Edge Shear Constraints*. Int. J. Num. Meth. Engrg., v. 26, 1988, p. 1101-1128.
20. REISSNER, E. *On the Theory of Bending of Elastic Plates*. Journal of Mathematics and Physics, v. 23, 1944, p. 184-191.
21. REISSNER, E. *The Effects of Transverse Shear Deformation on the Bending of Elastic Plates*. Journal of Applied Mechanics, v. 12, 1945, p. 69-77.
22. MINDLIN, R. D. *Influence of Rotatory Inertia and Shear on Flexural Motions of Isotropic, Elastic Plates*. Journal of Applied Mechanics, v. 18, 1951, p. 31-38.
23. MARGUERRE, K. *Zur Theorie Der Gekrummten Platte Grosser Formenderung*. Proc. 5th Internat. Congress of Applied Mechanics, 1938, p. 693-701.
24. MacNEAL, R. H., and HARDER, R. L. *A Proposed Standard Set of Problems to Test Finite Element Accuracy*. Proc. of 25th SDM Conf.: Finite Element Validation Forum, 1-41, Palm Springs, CA, 1984.
25. BELYTSCHKO, T., and LIU, W. K. *Test Problems for Shell Finite Elements*. Proc. of 26th SDM Conf.: Finite Element Standards Forum, Book 1, 25-44, Orlando, Florida, 1985.
26. SCORDELIS, A. C., and LO, K. S. *Computer Analysis of Cylindrical Shells*. J. Amer. Concr. Inst., v. 61, 1969, p. 539-561.
27. BATOZ, J. L. *An Explicit Formulation for an Efficient Triangular Plate-Bending Element*. Int. J. Numer. Meths. Engrg., v. 18, 1982, p. 1077-1089.
28. STOLARSKI, H., BELYTSCHKO, T., CARPENTER, N., and KENNEDY, J. M. *A Simple Triangular Curved Shell Element*. Engrg. Comput., v. 1, 1984, p. 210-218.
29. CARPENTER, N., STOLARSKI, H., and BELYTSCHKO, T. *A Flat Triangular-Shell Element with Improved Membrane Interpolation*. Commun. Appl. Numer. Meth., 1985.
30. OLSON, M. D., and BEARDEN, T. W. *A Simple Flat Triangular Shell Element Revisited*. Int. J. Numer. Meths. Engrg., v. 14, 1979, p. 51-68.
31. MORLEY, L. S. D., and MORRIS, A. J. *Conflict Between Finite Elements and Shell Theory*. Royal Aircraft Establishment, London, 1978.

DISTRIBUTION LIST

No. of Copies	To
1	Office of the Under Secretary of Defense for Research and Engineering, The Pentagon, Washington, DC 20301
1	Commander, U.S. Army Materiel Command, 5001 Eisenhower Avenue, Alexandria, VA 22333-0001 ATTN: AMCLD
1	Commander, U.S. Army Laboratory Command, 2800 Powder Mill Road, Adelphi, MD 20783-1145 ATTN: AMSLC-IM-TL
1	AMSLC-CT
2	Commander, Defense Technical Information Center, Cameron Station, Building 5, 5010 Duke Street, Alexandria, VA 22304-6145 ATTN: DTIC-FDAC
1	Metals and Ceramics Information Center, Battelle Columbus Laboratories, 505 King Avenue, Columbus, OH 43201
1	Commander, Army Research Office, P.O. Box 12211, Research Triangle Park, NC 27709-2211 ATTN: Information Processing Office
1	Commander, U.S. Army Electronics Technology and Devices Laboratory, Fort Monmouth, NJ 07703-5000 ATTN: SLCET-DT
1	Commander, U.S. Army Missile Command, Redstone Arsenal, AL 35898-5247 ATTN: AMSMI-RD-ST
1	Technical Library
2	Commander, U.S. Army Armament, Munitions and Chemical Command, Dover, NJ 07801 ATTN: SMCAR-TDC
1	Commander, U.S. Army Natick Research, Development and Engineering Center, Natick, MA 01760 ATTN: Technical Library
1	Commander, U.S. Army Tank-Automotive Command, Warren, MI 48397-5000 ATTN: AMSTA-R
1	Commander, U.S. Army Engineer Waterways Experiment Station, P.O. Box 631, Vicksburg, MS 39180 ATTN: Research Center Library
1	Director, U.S. Army Ballistic Research Laboratory, Aberdeen Proving Ground, MD 21005 ATTN: SLCBR-DD-T (STINFO)
1	SLCBR-IV-M, Dr. W. H. Drysdale
1	SLCBR-TB-W, Dr. J. Walter
1	SLCBR-TB-W, Dr. Thomas W. Wright
1	Director, Benet Weapons Laboratory, LCWSL, USA AMCCOM, Watervliet, NY 12189 ATTN: AMSMC-LCB-TL
1	Commander, U.S. Army Foreign Science and Technology Center, 220 7th Street, N.E., Charlottesville, VA 22901-5396 ATTN: AIAST-RA-ST
1	Commander, U.S. Army Aviation Systems Command, Aviation Research and Technology Activity, Aviation Applied Technology Directorate, Fort Eustis, VA 23604-5577 ATTN: SAVDL-E-MOS
1	Director, Langley Directorate, U.S. Army Air Mobility Research and Development Laboratory, NASA-Langley Research Center, Hampton, VA 23665 ATTN: Aerostructures Directorate
1	Naval Research Laboratory, Washington, DC 20375 ATTN: Code 5830
1	Office of Naval Research, 800 North Quincy Street, Arlington, VA 22217-5000 ATTN: Mechanics Division, Code 1132-SM

No. of Copies	To
1 1	Naval Air Development Center, Warminster, PA 18974-5000 ATTN: Code 6064 AVCSTD/6043
1	U.S. Navy David Taylor Research Center, Bethesda, MD 20084 ATTN: Code 172
1	U.S. Air Force Office of Scientific Research, Bolling Air Force Base, Washington, DC 20332 ATTN: Mechanics Division
1	Commander, U.S. Air Force Materials Laboratory, Wright-Patterson Air Force Base, OH 45433 ATTN: AFWAL/MLLN
1	National Aeronautics and Space Administration, Marshall Space Flight Center, Huntsville, AL 35812 ATTN: EH01, Dir, M&P lab
1	Committee on Marine Structures, Marine Board, National Research Council, 2101 Constitution Avenue, N.W., Washington, DC 20418
1 1	U.S. Army Research Office, P.O. Box 12211, Research Triangle Park, NC 27709 ATTN: Dr. Robert Singleton Dr. Gary L. Anderson, Chief, Structures and Dynamics Branch, Engineering Sciences Division
1	NASA - Langley Research Center, U.S. Army Aerostructures Directorate, USAARTA, Hampton, VA 23665-5225 ATTN: Dr. F. D. Bartlett, Jr., MS 266
1	NASA - Langley Research Center, Hampton, VA 23665 ATTN: H. L. Bohon, MS 243
1	George Washington University Center - at NASA - Langley Research Center, Hampton, VA 23665 ATTN: Professor A. K. Noor, Mail Stop 246C
1	NASA/GSFC, Greenbelt, MD 20771 ATTN: Mr. William Case, Mail Code 725
1	Ship and Submarine Materials Technology, DTRC-0115, Annapolis, MD 21402 ATTN: Mr. Ivan L. Caplan
1	Director, Structures Directorate, USA MICOM, Redstone Arsenal, AL 35898-5247 ATTN: AMSMI-RD-ST, Dr. Larry C. Mixon
1 1	Buret Laboratories, Watervliet Arsenal, Watervliet, NY 12189-4050 ATTN: Dr. Giuliano D'Andrea, Chief, Research Division Dr. John Vasilakis, Chief, Applied Mechanics Branch
1	Office of Naval Research, Solid Mechanics Program, 300 North Quincy Street, Arlington, VA 22217-5000 ATTN: Dr. Roshdy Barsoum, Code 1132
1 1	Massachusetts Institute of Technology, Department of Mechanical Engineering, Cambridge, MA 02139 ATTN: Professor K. J. Bathe Professor David Parks
1	Massachusetts Institute of Technology, Department of Astronautics and Aeronautics, Building 73, Room 311, Cambridge, MA 02139 ATTN: Professor Ted H. H. Pian
1	Professor S. N. Atluri, Director, Center for the Advancement of Computational Mechanics, Georgia Institute of Technology, Mail Code 0356, Atlanta, GA 30332
1	Dr. Lawrence C. Bank, The Catholic University of America, Department of Civil Engineering, Washington, DC 20064

No. of Copies	To
1	Professor Ted Belytschko, Northwestern University, Department of Civil Engineering, Evanston, IL 60201
1	Professor Fu-Kuo Chang, Stanford University, Department of Aeronautics and Astronautics, Stanford, CA 94305
1	Professor Tse-Yung P. Chang, The University of Akron, Department of Civil Engineering, Akron, OH 44325
1	Dr. Sailendra N. Chatterjee, Materials Sciences Corporation, Gwynedd Plaza II, Bethlehem Pike, Springhouse, PA 19477
1	Professor Thomas J. R. Hughes, Stanford University, Division of Applied Mechanics, Durand Building, Stanford, CA 94305
1	Professor S. W. Lee, University of Maryland, Department of Aerospace Engineering, College Park, MD 20742
1	Professor Alan J. Levy, Syracuse University, Department of Mechanical and Aerospace Engineering, 139 E. A. Link Hall, Syracuse, NY 13244-1240
1	Professor J. N. Reddy, Virginia Polytechnic Institute and State University, College of Engineering, Department of Engineering Science and Mechanics, Blacksburg, VA 24061-0219
1	Professor L. W. Rehfield, University of California at Davis, Department of Mechanical Engineering, Davis, CA 95616
1	Professor Eric Reissner, University of California at San Diego, Department of Applied Mechanics and Engineering Science, LaJolla, CA 92093
1	Professor John N. Rossettos, Northeastern University, College of Engineering, Department of Mechanical Engineering, 360 Huntington Avenue, Boston, MA 02115
1	Professor J. C. Simo, Stanford University, Division of Applied Mechanics, Stanford, CA 94305
1	R. L. Spilyer, Rensselaer Polytechnical Institute, Department of Mechanical Engineering, Aeronautical Engineering and Mechanics, Troy, NY 12181
1	Dr. G. M. Stanley, Lockheed Palo Alto Research Laboratory, Mechanics of Materials Engineering, Palo Alto, CA 94304
2	Director, U.S. Army Materials Technology Laboratory, Watertown, MA 02172-0001
1	ATTN: SLCMT-TML
1	Author

U.S. Army Materials Technology Laboratory
Watertown, Massachusetts 02172-0001
A C⁰-ANISOPARAMETRIC THREE-NODE SHALLOW
SHELL ELEMENT FOR GENERAL SHELL ANALYSIS -
Alexander Tessler

Technical Report MTL TR 89-72, August 1989, 19 pp-
ilus, D/A Project: 1L161102.AH42,
AMCMS Code: 61102A

A highly desirable three-node shallowly curved shell element is proposed for general shell analysis. Constrained-type C⁰-anisoparametric interpolations are derived for the membrane and transverse displacement fields by the use of explicit edge constraints. Pertinent issues on shell theory and finite element approximations are addressed. Several numerical studies are carried out which demonstrate the effectiveness of this new triangular element in the regime of thin and moderately thick shells.

AD UNCLASSIFIED
UNLIMITED DISTRIBUTION

Key Words

Shallow shell
Mindlin theory
Marguerre theory

U.S. Army Materials Technology Laboratory
Watertown, Massachusetts 02172-0001
A C⁰-ANISOPARAMETRIC THREE-NODE SHALLOW
SHELL ELEMENT FOR GENERAL SHELL ANALYSIS -
Alexander Tessler

Technical Report MTL TR 89-72, August 1989, 19 pp-
ilus, D/A Project: 1L161102.AH42,
AMCMS Code: 61102A

A highly desirable three-node shallowly curved shell element is proposed for general shell analysis. Constrained-type C⁰-anisoparametric interpolations are derived for the membrane and transverse displacement fields by the use of explicit edge constraints. Pertinent issues on shell theory and finite element approximations are addressed. Several numerical studies are carried out which demonstrate the effectiveness of this new triangular element in the regime of thin and moderately thick shells.

AD UNCLASSIFIED
UNLIMITED DISTRIBUTION

Key Words

Shallow shell
Mindlin theory
Marguerre theory

U.S. Army Materials Technology Laboratory
Watertown, Massachusetts 02172-0001
A C⁰-ANISOPARAMETRIC THREE-NODE SHALLOW
SHELL ELEMENT FOR GENERAL SHELL ANALYSIS -
Alexander Tessler

Technical Report MTL TR 89-72, August 1989, 19 pp-
ilus, D/A Project: 1L161102.AH42,
AMCMS Code: 61102A

A highly desirable three-node shallowly curved shell element is proposed for general shell analysis. Constrained-type C⁰-anisoparametric interpolations are derived for the membrane and transverse displacement fields by the use of explicit edge constraints. Pertinent issues on shell theory and finite element approximations are addressed. Several numerical studies are carried out which demonstrate the effectiveness of this new triangular element in the regime of thin and moderately thick shells.

AD UNCLASSIFIED
UNLIMITED DISTRIBUTION

Key Words

Shallow shell
Mindlin theory
Marguerre theory

U.S. Army Materials Technology Laboratory
Watertown, Massachusetts 02172-0001
A C⁰-ANISOPARAMETRIC THREE-NODE SHALLOW
SHELL ELEMENT FOR GENERAL SHELL ANALYSIS -
Alexander Tessler

Technical Report MTL TR 89-72, August 1989, 19 pp-
ilus, D/A Project: 1L161102.AH42,
AMCMS Code: 61102A

A highly desirable three-node shallowly curved shell element is proposed for general shell analysis. Constrained-type C⁰-anisoparametric interpolations are derived for the membrane and transverse displacement fields by the use of explicit edge constraints. Pertinent issues on shell theory and finite element approximations are addressed. Several numerical studies are carried out which demonstrate the effectiveness of this new triangular element in the regime of thin and moderately thick shells.

AD UNCLASSIFIED
UNLIMITED DISTRIBUTION

Key Words

Shallow shell
Mindlin theory
Marguerre theory